Suitable Waves for Bender Element Tests: Interpretations, Errors and Modelling Aspects

Muhammad E. Rahman^{1*}, Vikram Pakrashi², Subhadeep Banerjee³ and

Trevor Orr⁴

^{1*}Senior Lecturer, School of Engineering and Science, Curtin University Sarawak, Malaysia. E-mail: merahman@curtin.edu.my, B.E, M.Eng.Sc, PhD
²Lecturer, Dynamical Systems and Risk Laboratory, Department of Civil and Environmental

Engineering, <u>School of Engineering</u>, University College Cork, Ireland. E-mail: V.Pakrashi@ucc.ie, B.E, PhD, CEng, MIEI

³Assistant Professor, Department of Civil Engineering, Indian Institute of Technology – Madras, India. E-mail: subhadeep@iitm.ac.in, B.E, PhD

⁴Associate Professor, Department of Civil, Structural and Environmental Engineering, Trinity College Dublin, Ireland. E-mail: torr@tcd.ie, BA, BAI, MSc, PhD, MICE, CEng, FIEI, EurIng

Suitable Waves for Bender Element Tests: Interpretations, Errors and Modelling Aspects

Abstract: Extensive research on bender element tests has been carried out by many researchers but precise guidelines for carrying out such tests have not yet been established. It is often recommended that, when using a particular bender element test for the first time on a particular soil to determine its small strain dynamic properties, several methods should be tried and the results compared in order to improve confidence in the results obtained. Demonstrated use of relatively easy analytical models for investigating different scenarios of bender element testing is another aspect that should be further looked into. This paper presents laboratory experiments and dynamic finite element analyses to determine a suitable wave for use in bender element tests in the laboratory to measure small strain shear stiffness (G_{max}). The suitability of a distorted sine wave over a continuous sine wave for tests is observed from laboratory experiments and dynamic finite element analyses. The use of simple finite element models for assessing a number of aspects in relation to bender element testing is demonstrated.

Keywords: Bender Element Test, Numerical Analysis, Sine Wave, Small Strain Shear Stiffness

1. Introduction

Dynamic analyses to evaluate the small strain stiffness of soil and the response of earth structures to dynamic stress applications are finding increased popularity in civil engineering practice. Idealised models and analytical techniques may be used to represent a soil deposit and its response in this regard. Estimation of the small strain stiffness and the dynamic properties of the soil are important and challenging problems. Precise measurement of the small strain stiffness and dynamic soil properties are difficult tasks when analysing dynamic geotechnical engineering problems (Kramer, 1996). Several field and laboratory techniques are available to measure the dynamic properties, many of which involve measurements at small-strain (Sorensen et. al., 2010, Yamashita et. al., 2009) or large strain levels (Salgado et. al., 1997). The choice of a particular technique depends on the specific problem to be solved. The existing tests provide insights into correlation with other tests methods, with types of specimens or the methods, but the requirement of more data and the approaches towards rapid modelling of scenarios still remain a topical subject,

Some key soil properties that influence wave propagation and other low-strain phenomena include stiffness, damping, Poisson's ratio and density. Of these, stiffness and damping are the most important since the others usually have less influence and tend to fall within relatively narrow ranges (Kramer, 1996). Laboratory tests are available to measure dynamic properties of soils at small strain levels. The resonant column test (Youn et.al, 2008), ultrasonic pulse test (Weidinger et. al., 2009), and bender element test (Fonseca et.al, 2009) are the commonly employed techniques to measure small strain stiffness and dynamic properties. Extensive research on bender elements test has been carried out by many researchers in last few decades (Jovicic et al., 1996, Arulnathan et. al., 1998, Arroyo et. al., 2003 and Arroyo et. al., 2006) but precise guidelines for carrying out such tests are not completely established. It is usually recommended to try and compare several methods when using a particular test for the first time on a particular soil to determine its small strain stiffness and dynamic properties, in order to improve confidence in the results obtained (Jovicic et. al., 1996 and Arulnathan et. al., 1998). Theoretical analysis and experimental validation in the frequency domain have been recently carried out (Alvarado and Coop, 2011) using a transfer function to characterise different soils with linear, but dispersive characteristics of soil in relation to the waves. A wavelet based approach for singularity detection has also been proposed recently by Bonal et. al., (2012) in connection with assessment of shear wave arrival time. Essentially, the use of bender elements to predict shear modulus is a system identification problem fraught with different levels of variability, noise, method of assessment, inherent uncertainties in soil characteristics, type of instrument used and the level of analytical effort. Investigations into these aspects remain topical and important (El-Sekelly et. al., 2013) in this regard.

This paper considers the suitability of different waves for bender element tests for various situations and also assesses the variability of such results acknowledging the typical resources available for experimental and analytical studies. Initially, experiments are carried out on marine clay in Chennai, India with sinusoidal excitation to obtain the variability of estimated shear modulus. The study is augmented with investigation on boulder clay, Dublin, Ireland and the suitability of distorted sine wave as an excitation in investigated. Traditional theoretical modelling is taken up next to demonstrate that even a

relatively simple finite element model address a number of issues related to the estimation, capturing a number of observations observed experimentally. The study adds to the on-going understanding of the different approaches towards the estimation of shear modulus using bender elements in the presence of varied methods, equipment and analytical rigour.

2. Bender Elements

Bender elements have been used for the measurement of elastic small strain stiffness and damping ratio in a triaxial cell. The bender element technique has undergone significant development in the last few decades (Dano and Hicher, 2002). In the early stage, piezoceramics were mainly used to generate and receive compression P-waves. Since little information about the soil structure can be obtained from P-waves and since the P-wave velocities are highly influenced by the pore fluid, the piezoceramics have been combined in different forms to generate and receive shear waves. Such combined forms of piezoceramic are used in gauges for measuring vibrations known as bender elements (Brocanelli & Rinaldi, 1998 and Karl et. al., 2003).

Bender elements consist of two thin piezoceramic plates rigidly bonded to a central metallic plate. Two thin conductive layers, which serve as electrodes, are glued externally to the bender element. The polarization of the ceramic material in each plate and the electrical connections are such that when a driving voltage is applied to the element, one plate elongates and the other shortens. When the measurement of the shear wave velocity is made using bender elements in the triaxial test apparatus, one bender element is fixed in place in the top cap and the other in the pedestal. The elements are of 1 mm thickness,

12 mm width and about 15mm length. In the set-up in the triaxial cell, the bender elements at both ends protrude into the specimen as cantilevers. When the bender element at the top is set into motion, the soil surrounding the bender element is forced to move back and forth horizontally and its motion initiates the propagation of a shear wave through the soil sample. When the shear wave reaches the other bender element at the other end of the specimen in the triaxial apparatus, it causes it to bend and thus produce a voltage. This output signal can be captured through an oscilloscope and the travel time determined by measuring the time difference between the input and the output signals. The shear wave velocity can be found by dividing the travel distance, L, by the travel time, t where the travel distance of the wave is taken to be equal to the specimen's length minus the protrusion of the two-bender elements at the both ends. After determining the propagation shear wave velocity it is possible to calculate the small strain shear modulus, G_{max} , by the elastic continuum mechanics relationship

Where ρ is the soil density and v_s is the shear wave velocity.

The damping ratio, ξ , can be determined from the frequency response curve using the half-power bandwidth method. The half-power bandwidth method is a very common method for measuring damping (Clough and Penzien, 1993) and uses the relative width of the response spectrum.

The advantages of bender elements are that they can also be incorporated into the oedometer test apparatus and simple shear test device. However, normally they are incorporated into the triaxial apparatus (Karl et. al., 2003, Ishihara, 1996 and Kramer, 1996). Anisotropy of the soil stiffness can also be investigated by locating bender

(1)

(1)

elements on two vertical and opposite sides of a sample. The disadvantage of the bender element is that the element must be waterproofed to prevent short circuits, which is often difficult to achieve when testing dense or hard saturated materials. Insertion of the bender element into such hard materials can easily damage the sealing for waterproofing (Ishihara, 1996).

The shear modulus of soil is related to the shear wave velocity determined using a bender element test. The bender element induces very small strains which lie typically within the elastic limit. Dyvik & Madshus (1985) estimated the maximum shear strain induced by bender elements to be less than 0.001%, so that G_{max} is relevant for very small strain (Brignoli et al., 1996 and Karl et al., 2003). Jovicic (1997) validated the assumption of elasticity experimentally by finding that there was no volume change in specimens when drained bender element tests were performed. No pore water pressure was generated when undrained tests were carried out.

Although the use of the bender element apparatus is simple, the application of bender element test for the measurement of small strain stiffness and the damping ratio may not be straightforward as it is difficult to measure the exact travel time between the input and output signals. The strain level induced by the bender element test is directly proportional to the displacement at the tip of the bender element so that it is difficult to measure. Determination of the shear wave velocity is a key element for establishing G_{max} in bender element tests. The shear wave velocity is directly related to the shear wave travel distance and the travel time and is calculated by dividing the travel distance by the travel time. Initially there was some doubt as to what should be taken as the true travel distance. researchers thought it might be the full height of the sample. Viggiani and Atkinson (1995a) carried out some laboratory tests on a set of reconstituted samples of Speswhite kaolin of different lengths to investigate what should be taken as the travel distance. Travel times are plotted against the overall length of the sample for different confining stress state conditions. The test data fall on straight lines, each with an intercept of about 6 mm on the vertical axis where the bender elements used for those tests were 3 mm long. From these tests it has been concluded that the travel wave distance should be between the tips of the elements rather than the full length of the sample. This is in agreement with previous experimental work by Dyvik and Madshus (1985).

Consequently, the most important parameter to be determined in a bender element test is the exact travel time of the shear wave between the transmitter and the receiver. Actually the principal problem with the bender element test has always been the subjectivity of the determination of the arrival time used to calculate shear wave velocity (Jovicic et al., 1996 and Lee & Santamarina, 2004). The travel time is dependent on the shape of the wave transmitted through the soil sample. The procedure commonly used in bender element tests is to generate a square wave and to determine the time of first arrivals (Jovicic et al., 1996 and Viggiani & Atkinson, 1995a) although there is considerable distortion of the output signal using a square wave. The problem with the square wave is that it is composed of a wide spectrum of frequencies (Jovicic et al., 1996). From the received signal of the square wave alone, it is uncertain whether the shear wave arrival is at the point of first deflection, the reversal point, or some other point.

To reduce the degree of subjectivity in the interpretation, and to avoid the difficulty in interpreting the square wave response, Viggiani and Atkinson, (1995a) suggested using a

sine pulse as the input signal. Consisting of a single frequency, the output wave is generally of a similar shape to the input signal, but it is still very difficult to determine the travel time. The problem arises due to a phenomenon called the near field effect. The near field effect is caused by the very rapid P-waves that mask the first arrivals of the, slower, S-waves. The near field effect may mask the arrival of a shear wave when the distance between the source and the receiver is within the range of 1/4 to 4 wavelengths. This is the situation in bender element tests where the distance between the transmitter and the receiver is relatively small and is about 2 to 3 wavelengths (Viggiani and Atkinson, 1995a). Brignoli & Gotti (1992) also found the existence of near field effects in bender element tests and these have been further investigated by Jovicic et al. (1996). The wavelength can be estimated from:

$$\lambda = \frac{v_s}{f}$$

Where, f is the frequency of the input signal in Hertz.

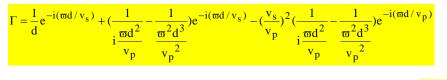
Jovicic et al., (1996) derived an analytical solution for the time record at a point resulting from the equation for the excitation by a transverse sine pulse of a point source within an infinite isotropic elastic medium, obtained by Sanches-Salinero et al., 1986. The fundamental solution for the transverse motion S (Sanches-Salinero et al., 1986) is

(2)

given in the form

$$\mathbf{S} = \frac{1}{4\pi \alpha v^2} \Gamma \tag{3}$$

where the function Γ is given by:



(4)

where d is the distance between the transmitter and receiver of bender element, v_s is shear wave velocity, v_p is primary wave velocity and ω the angular velocity. From Equation 4, it can be seen that there are three coupled components to the transverse motion, which comprise both the near field and far field effects. This is because the motions of the elements are not pure compressive or shear motions (Brignoli et al. 1996) and generally some compressive or shear motion occurs. All three terms represent transverse motion. While they propagate with different velocities, the first two travel with the velocity of a shear wave, and the third travels with the velocity of a compression wave. The attenuation occurs at different rates with geometrical damping for the three components, the second and third terms attenuating at a rate an order of magnitude faster than the first term. The coefficient of the first term is proportional to the inverse of the distance and the coefficients of second and third terms are proportional to the inverse of square of the distance and the cube of the distance, which implies that the last two terms are only significant for small distances and are called near field terms and first term is significant for larger distances and is called the far field term. In bender element tests, the effect is amplified by the S-wave source and substantial P-wave energy that is often developed.

Sanches-Salinero et al. (1986) expressed their results in terms of the ratio d/λ , where λ is the wavelength of the input signal. Later Jovicic et al. (1996) denoted this ratio as R_d . The value of R_d represents the number of wave lengths that occur between the bender

element transmitter and receiver and which control the shape of the received signal through the degree of attenuation of each term of Equation 4 that occurs as the wave travels through the sample. R_d is calculated from:

$$\mathbf{R}_{\mathbf{d}} = \frac{\mathbf{d}}{\lambda} = \frac{\mathbf{d}\mathbf{f}}{\mathbf{v}_{\mathbf{s}}} \tag{5}$$

For low values of R_d there is an initial downward deflection of the trace before the shear wave arrives, representing the near field effect given by the third component of equation 4. For high values of R_d the near field effect is almost absent. Jovicic et al. (1996) carried out a series of experiments using bender elements on Speswhite kaolin specimens with an isotropic effective stress of 200 kPa and values of R_d of 1.1 and 8.1. The results confirmed that for low R_d values the near field effect dominates, while for high R_d values the near field effect is almost insignificant. The authors recommended selecting a high enough frequency so that the soil being tested has a high R_d ratio. In practice this cannot be always achieved, because at the high frequency required for stiffer materials, overshooting of the transmitting element can occur. These experiments were carried out on cemented granular soft rock, with G_{max} of 2.5 GPa at an effective stress of 200 kPa. At 2.96 kHz the element follows perfectly the input wave, while at 29.6 kHz it does not and overshooting occurs. The limiting frequency at which overshooting starts to occur depends on the relative impedances of the soil and the element and overshooting is found to be severe for stiffer soil as well as being pronounced for square waves.

3. Bender Element Tests

The following section details the results of bender element tests which would be later used for performance evaluation of numerical simulations. The first series of tests were conducted on Chennai marine clay. Some basic properties of Chennai marine clay for all the tests are shown in the Table 1.

Table 1: Basic Properties of Chennai Marine Clay

Liquid limit	54%
Plastic limit	30%
Sand	10%
Silt	34%
Clay	56%

The bender element tests were carried in the triaxial chamber to simulate the field confining pressure. The transmitter element is mounted at the pedestal of the triaxial chamber. The receiver element is inserted on the top of the soil sample. Electric pulses are applied to the transmitter through the wave-form generator. The continuous shear waves, thus produced, would travel through the soil sample before being recorded by the receiver at the other end. By measuring the travel time (t) and the distance (L) between the tips of the bender elements, the shear wave velocity (v_s) can be obtained as,

$$v_s = L/t \tag{6}$$

The maximum shear modulus can thus be computed as,

$$G_{\max} = \rho v_s^2 \tag{7}$$

Where ρ is the density of the soil.

The estimation of maximum shear modulus obtained in this regard is shown in Table 2.

		Maximum shear modulus (MPa)			
Sl.no.	Shear wave		Field data		
		From Bender	from	From Viggiani and	
	velocity (m/sec)	Element tests	Boominathan	Atkinson (1995)	
		(MPa)	et al. (2008)	(MPa)	
			(MPa)		
BET-1	91	15.39		Range: 15 – 40	
BET-2	85	13.43		(Depending on	
BET-3	93	16.08	17	plasticity and	
BET-4	87	14.07		mineralogy of the cohesive soil)	

 Table 2: Summarizes the Shear Wave Velocity and Maximum Shear Modulus Obtained for Chennai Marine Clay.

The results presented in Table 2 establish the repeatability of the estimates and the control of the test. The observed shear wave velocities and corresponding maximum shear modulus are in accordance with the results obtained from field tests on Chennai Marine clay, as reported by Boominathan et. al. (2008). Moreover the range of maximum shear modulus obtained for Chennai marine clay was found to be comparable with the predictions computed from empirical correlations proposed by Viggiani and Atkinson (1995) for clays with different mineralogy.

The typical input signal and receiver output from a bender element test on Chennai marine clay is shown in the Figure 1. It should be noted that the raw data of the receiver output generally contain noises of high frequencies. As it is well-understood that the resonant frequency of marine cannot have resonant frequency greater than 10Hz, a low pass filter with cut-off frequency of 10Hz is used to remove the spurious signals. It should also be noted that the travel time and thus the shear wave velocity are computed from the first few signals, beyond which reflection of the waves may incur uncertainty in

the measurements (Ishihara, 1996). While this is associated with some subjectivity in the analysis, it also opens up the possibility of investigating the suitability of relatively rapidly created axisymmetric models for estimation of maximum shear modulus using bender elements and further analyses related to the suitability of the input waves.

It is well-established that the soil type, experimental techniques and conditions influence the measurement of maximum shear modulus (Viggiani and Atkinson, 1995a,b; Ishihara, 1996). Viggiani and Atkinson (1995b) indicated that the maximum shear modulus of the natural clay may substantially vary from that of the reconstituted clay. Consequently, it was deemed important to compare with tests on other types of clay in relation to the suitability of the input waves.

Bender element tests using a Wykeham-Farrance 100mm triaxial cell were carried out on Dublin boulder clay with cylindrical specimens of 200mm length and 100mm diameter bender elements in the top cap and base pedestal. A Thurlby Thander TGA 1240 function generator, a Pico ADC-212 high-resolution oscilloscope and shielded output cables were also used. The excitation signal, produced by a function generator was amplified and sent to the bender element in the top cap with maximum peak-to-peak amplitude of 20 V. The waves transmitted through the soil specimen from the top were recorded at the base by the receiver and displayed on an oscilloscope. Calibration was carried out by placing the two platens in direct contact and measuring the time interval between the initiation of the electrical impulse sent to the transmitter and the initial arrival of the waveform recorded at the receiver. The top platen was marked with respect to the base platen in order to avoid ambiguity in test interpretation (Lawler, 2002). The measured waveforms and calibration times obtained for the bender elements were checked to ensure that there was no time lag. The absence of wave transmission paths, other than through the soil specimen, was checked as well by placing the two platens in the triaxial cell without any soil and without contact and ensuring that no wave arrival was recorded by the receiver when pulses were generated by the transmitter. Average properties of Dublin boulder clay are shown in the Table 3. Bender element measurements were carried out by exciting a transmitter with a standard sine waves and arbitrarily distorted sine waves, followed by detection of the first arrival of the waves at the receiver. Signals were sent top down, from the top cap to the base. Lings and Greening (2001) found that there was no difference between the signals when they were sent top down or bottom up. Input and output traces of a standard sine wave (Figure 2) and an arbitrary distorted sine wave (Figure 3) indicate the presence of a near-field effect for a sine wave and the absence of such an effectfor a distorted sine wave.

Parameter	Upper Brown	Upper Black	Lower Brown	Lower Black
Moisture content, %	13.1	9.7	11.5	11.3
Bulk density, Mgm ⁻³	2.228	2.337	2.283	2.284
Liquid limit, %	29.3	28.3	30.0	29.5
Plastic limit, %	15.9	15.1	14.9	17.8
Plasticity index, %	13.4	13.2	15.1	11.8
Clay content, %	11.7	14.8	17.8	17.5
Silt content, %	17.0	24.7	28.3	30.5
Sand content, %	25.0	24.7	25.7	34.0
Gravel content, %	46.3	35.8	28.0	35.5

Table 3: Summary of average basic material properties (Skipper et al., 2005)

As discussed in this section, there remains an interesting possibility in investigating the use of traditional axisymmetric models for assessing shear modulus from bender elements

and a number of observations were made from such simpler modelling, in relation to the experimental evidences.

4. Investigations into the Usefulness of Traditional Axisymmetric Finite Element Models

4.1 Finite Element Method and Model

Finite element method (FEM) is a numerical technique for finding approximate solutions of engineering problems. Mathematically, differential equations or integral expression can be used to describe engineering problem. Individual finite elements can be pictured as small pieces of a body. Elements are connected at points called nodes. The assembly of elements is called a finite element body. The particular arrangement of elements is called mesh. Numerically, an FE mesh is represented by a system of algebraic equations to be solved for unknowns at nodes (Cook et. al., 2002). The basic steps of an FEA are as follows (Stasa, 1985; Bathe, 1982 and Cook et. al., 2002):

 Problem identification and discretization: that subdivide the problem into nodes and elements.

Selection of an interpolation function to represent the physical behaviour of an element; that is an approximate continuous function as assumed to represent the behaviour of an element.

Development of the displacement equation for each element.

 Assembly of the elements to represent the entire problem and construction of the global stiffness matrix.

Application of the boundary conditions, initial conditions and loading.

 Solution of a set of linear or non-linear algebraic equations simultaneously to obtain nodal results, such as displacement values at different nodes.

 Use of the nodal values and interpolation functions to determine other parameters such as stress, strain and velocity etc. inside each element.

Commented [v1]: I think not needed – delete. Just give details of this model.

In this paper, a Finite Element (FE) model is developed to calculate the time gap between the transmitted wave and the received wave in the cylindrical triaxial cell sample. The problem is three-dimensional in nature but a simplified model consisting of twodimensional plane strain, linear-elastic finite element analyses were deemed sufficient and carried out using the commercially available general-purpose finite element package PLAXIS. The soil was modelled using a 15-noded plane strain triangular element. For a 15-node triangle the order of interpolation for deflections is four and the integration involves 12 stress points. The dimensions of the finite element mesh (Figure 4) used to model the bender element were 225mm high and 100mm wide. The behaviour of the bender elements is modelled by use of a 5 noded beam element that represents real plates in the out-of-plane direction and the interface between the soil and the bender elements was characterized as an interface element. The beam elements are based on Mindlin's beam theory, which allows for beam deflections due to shearing as well as bending. The bender element top cap was modelled by use of a 15-noded triangular element and the interface between the soil and the top cap was characterized as an interface element. The boundary conditions were applied by selecting the standard fixities, which meant that the horizontal top and bottom boundaries (Figure 4) were fully fixed and the side boundaries

were kept stress free to replicate the actual test condition (Arulnathan et. al., 1998). The load and boundary conditions and triangular mesh are also shown in Figure 4. In the analyses, the input voltage signal applied to the transmitting bender element was modelled by means of a transverse sinusoidal motion with an amplitude of 1.0×10^{-3} mm, which acted at a point representing the tip of the transmitter. Based on the assumption of plane wave fronts and the absence of any reflected or refracted waves, the output voltage signal from the receiving bender element was taken from the tip of the receiver and the travel time of a shear wave between the transmitter and the receiver were taken as the time between characteristic points in the signals recorded at these two points. The most commonly used characteristic points are the first peak, first trough or zero crossing of the input and output signals. The travel time between two points can be taken as the time shift that produces the peak cross-correlation between signals recorded at these two points (Arulnathan et. al., 1998).

4.2 Model Properties

The Poisson's ratio (v) chosen for the soil was 0.495, replicating undrained condition of the soil. The shear wave velocity of soil was calculated as 386.2 m/s using:

$$v_s = \frac{\sqrt{E_{max}}}{\sqrt{2\rho(1+\nu)}} = \sqrt{\frac{G_{max}}{\rho}}$$
(8)

Where ρ , the soil density is equal to 2242 kg/m³ and E_{max}, the small strain undrained Young's modulus is equal to 1GPa. This value is a typical E_{max} value obtained from laboratory tests on Dublin Boulder Clay.The bender elements and top cap were made of lead zirconate and aluminium with small strain Young's moduliof 70GPa and 65GPa, densities of 2700kg/m³ and 7500kg/m³ and Poisson's ratios of 0.33 and 0.3 respectively.

4.3 Comparative Study between Plane Strain Elements and Axisymmetric Elements

A comparison between the results of the FE analyses using plane strain elements and axisymmetric elements help determine the type of element more suitable for the purpose since the real situation is neither a purely plane strain problem nor a purely axi-symmetric problem. Sine waves of 2098Hz and 10489Hz, along with an assumed input G_{max} of 334.45MPa were used. The shear wave velocity was calculated using $v_s = L/t$. The G_{max} values were calculated using Equation 1.The percentages errors in G_{max} were calculated with respect to the input G_{max} value (Table 4) and the lower percentage errors for the plane strain elements indicated that these were more suitable.

Frequency, Hz	% G _{max} error			
	Plane strain elements	Axi-symmetry elements		
2098	+4.57	-19.5		
10489	+1.32	-25.2		

Table 4- A Comparative Study of Plane Strain and Axisymmetric Elements

4.4 Effects of Mesh Dimension

An investigation of the G_{max} values obtained using different mesh dimensions indicated that the error in the predicted wave velocities increases exponentially with increase in the mesh dimensions. The percentage of errors in G_{max} due to using very fine, fine, medium and coarse meshes (corresponding to approximately 1000, 500, 250 and 100 elements respectively) were 0.55%, 0.97%, 2.7% and 5.5% respectively. For the subsequent analyses, very fine mesh densities were selected. However, even medium mesh is observed to give reasonable results.

4.5 Estimation using Single Sine Wave

A single sine wave (Figure 5) in the transverse direction at the tip of the transmitter bender element was used as an input signal to cause a deflection of the bender elements and to generate a wave through the soil to the receiver. A series of finite element analyses was carried out for different values of $R_d = \frac{d}{\lambda} = \frac{df}{v_s}$ between 1 and 8. The frequency range was 2.1kHz to 16.78kHz. The experimental output signals (Figure 6) from the receiver were analysed to obtain the G_{max} deviation percentages for different R_d values (Figure 7) by comparing the predicted G_{max} values obtained from the predicted shear wave velocity (v_s) at different R_d values with an assumed G_{max} value of 334.45 MPa. The G_{max} deviations were obtained using a number of methods to predict the shear wave arrival time. The first inflexion method yields deviations of the order of 4.57%, 3.8% and 2.6% for the R_d ratios of 1, 2 and 3 respectively, while for the remaining R_d values the percentage deviations are less than 2%. The percentage deviations obtained using the first peak-to-peak input and output waves method are 6.2% and 3.89% for the R_d ratios of 1, and 2 respectively, while for the remaining R_d values the percentage errors are less than or around 3%. The percentage deviations obtained using the cross correlation method are 5% and 9% for the R_d ratios of 1, and 2 respectively, while for the remaining R_d values the percentage deviations are less than or around 2%. In summary, there is a significant similarity between the G_{max} values obtained using the three interpretation methods and

when the R_d values are 1 and 2, the G_{max} percentage deviation is higher than 3.5% while it is less than 3.5% for R_d values from 3 to 8. This suggests that the true shear wave arrival time is masked by deviations due to near-field effects, as the predicted and theoretical arrival times are not the same. The potential sources of deviations reduce as R_d increases. The predicted G_{max} percentage deviations are presented in Table 5. The distance between the tips of the transmitter and the receiver was 184mm and the shear wave velocity of the soil was 386.6 m/s. The predicted shear wave arrival time corresponds to the theoretical arrival time of 0.476ms. The theoretical shear wave arrival time was not obtained using the output from the receiver because there was an initial downward deflection of the output signal due to the near-field effect. The input frequency has a significant influence on the near-field effect and this effect is not discernible when frequency is increased. Jovicic *et al.*, (1996) has also found similar trends. These results demonstrate the need to carry out a series of tests with different input frequencies in order to eliminate the nearfield effects.

Frequency, KHz	R_d	Predicted arrival time, ms	v _s , m/s	Predicted G _{max,} MPa	Calculated G _{max,} MPa	% deviation
2.1	1	0.492	373.98	313.57	334.45	6.24
4.2	2	0.486	378.60	321.37	334.45	3.91
6.3	3	0.480	383.33	329.45	334.45	1.49
8.4	4	0.483	380.95	325.37	334.45	2.71
10.5	5	0.483	380.95	325.37	334.45	2.71
12.6	6	0.484	380.17	324.03	334.45	3.12
14.7	7	0.480	383.33	329.45	334.45	1.49
16.8	8	0.479	384.19	330.92	334.45	1.06

Table 5– Percentage error in G_{max} predicted from shear wave velocity.

4.6 Estimation using a train of five Sinusoidal Waves

With unchanged mesh, boundary and material properties, a train of five sinusoidal waves (Figure 8) was used next in the transverse direction at the tip of the transmitter, in FE analyses with R_d values between 1 and 8. The shear wave outputs (Figure 9) and the G_{max} errors (Figure 10) indicate that the G_{max} values obtained using the first inflexion interpretation method are 17.4%, 4.6%, 3.74% and 3.3% for R_d ratios of 1, 2, 3 and 4 respectively while for remaining R_d values the percentage errors are less than 2%. The results of the analyses using the first peak-to-peak input and output wave method with an R_d ratio of 1 give higher percentage errors while the remaining results give reasonably consistent errors of between 1.37 and 2.6 percent for the calculated G_{max} . The single sine and the continuous sine signals behave very similarly with respect to the initial downward deflection. The results obtained using the continuous sine wave indicate that errors due to (i) wave interference at the boundary, (ii) the near-field effect and (iii) a non-one-dimensional wave travel mask the true shear wave arrival time. The second and third sources of error reduce as the input frequency, i.e. R_d increases.

4.7 Estimation using a Distorted Sine Wave

A single distorted sine wave (Figure 11), instead of a single standard sine wave in the transverse direction at the tip of the transmitter was examined next as an input signal. The calculated G_{max} value is strongly dependent on the amplitude ratio (Arroyo *et al.* (2003), which is the ratio between the amplitude of the first upward cycle to the amplitude of the second downward cycle. Jovicic *et al.* (1996) recommended that the amplitude of the first upward cycle of the wave should be reduced so as to cancel out the near-field effect. A

parametric study was carried out to examine the effect of this ratio on the initial deflection. Analyses carried out using amplitude ratios of 1/1.5, 1/2, 1/3, and 1/4 and the initial deflection values were normalised with respect to the initial deflection value for an amplitude ratios of 1/3. The output waves (Figure 12) indicate that the near-field effect reduces as the amplitude of the first upward cycle of the wave decreases and is zero when the cycle ratio is 1/3. The normalised deflection decreases with reducing cycle ratio up to 0.33 before increasing. The amplitude ratio of first upward cycle to the first downward cycle of the waves can be chosen so as to significantly cancel out the near-field effect. Consequently, the distorted sine wave is favourable for avoiding the problem of the near-field effects and determining the first arrival time as compared toa single sine wave or a continuous sine wave.

5. Conclusions

Extensive research on bender elements test has been carried out by many researchers in last few decades but precise guidelines for carrying out such tests have not yet been established. It is usually recommended to try and compare several methods when using a particular test for the first time on a particular soil to determine its small strain dynamic properties, in order to improve confidence in the results obtained (Jovicic et. al., 1996 and Arulnathan et. al., 1998).

The investigations presented in this paper suggest that in addition to the soil types, the choice of input signal in bender element tests may influence the determination of G_{max} . The effects of the input signal type on the G_{max} for a particular soil can be determined using finite element analysis and laboratory experiment. However it is expensive, time

consuming and need more sample to determine the suitable wave for a particular soil using laboratory experiment than finite element analysis. Based on this study it is concluded that for a particular soil it better to conduct finite element analysis to select suitable wave and then conduct laboratory experiment using best wave to determine the G_{max} .

A distorted sine wave is observed to be more favourable than a single standard sine wave or a train of sine waves due to its superior ability for cancelling out the near-field effect. The near-field effect is dependent on the ratio between the amplitudes of the first upward wave to the first downward wave of the input signal (R_d). The G_{max} values obtained from single standard sine and continuous sine waves presented in this study suggest that if the R_d ratio is 3 or above, the near-field effect does not significantly influence the measured travel time. However it was noted that for low values of R_d there is an initial downward deflection of the trace before the shear wave arrives, representing the near-field effect.

A comparison between the results of FE analyses using plane strain elements and axisymmetric elements have been carried out and it is found that the plane strain elements yield better results compared to axisymmetric elements. When using relatively simple FE models, employing fine mesh sizes were observed to yield the best results, although acceptable results can be obtained rapidly to investigate different testing scenarios even when a medium mesh size is considered.

Acknowledgements:

The authors gratefully acknowledge the involvement and help of the following: Department of Civil Engineering, University of Dublin, Trinity College. Nishimatsu Construction Co., Ltd

The Geotechnical Trust Fund of the Institution of Engineers of Ireland

References

Alvarado, G. and Coop, M.R. (2011), "On the performance of bender elements in triaxial tests", Géotechnique, 62(1), 1-17.

Arroyo, M.; Muir Wood, D. and Greening, P. D. (2003). "Source near-Field Effects and Pulse Tests in Soils Samples" Géotechnique, 53(3), 337-345.

Arroyo, M., Muir Wood, D., Greening, P. D., Medina, L. and Rio, J. (2006). "Effects of Sample Size on Bender-Based Axial G0 Measurements" Géotechnique, 56(1), 39-52.

Arulnathan, R., Boulanger, R.W. and Riemer, M. F, (1998), "Analysis of bender element tests", ASTM Geotechnical Testing Journal, 21(2), 120-131.

Bathe, K. J. (1982.), "Finite Element Procedures in Engineering Analysis", Englewood Cliffs; London, Prentice-Hall.

Bonal J., Donohue S. and McNally C. (2012). "Wavelet Analysis of Bender Element Signals", Géotechnique, 62(3), 243-252.

Boominathan A., Dodagoudar G. R., Suganthi A. and Maheswari R. U.(2008)."Seismic hazard assessment of Chennai city considering local site effects". J. Earth Syst. Sci. 117, S2, 853–863

Brignoli, E.G.M., Gotti, M., and Stokoe, K. H., (1996), "Measurement of shear waves in laboratory specimens by means of piezoelectric transducers", ASTM Geotechnical Testing Journal, 19(4), 384-397.

Brocanelli, D. and Rinaldi, V., (1998), "Measurement of low-strain material damping and wave velocity with bender elements in the frequency domain", Canadian Geotechnical Journal, 35(6), 1032-1040.

Clough, R.W. and Penzien, J. (1993). Dynamics of Structures. McGraw-Hill Book Co., Singapore.

Cook, R. D., Malkus, D. S., Plesha, M.E. and Witt, R. J., (2002), "Concepts and applications of finite element analysis", 4th ed, New York, John Wiley and Sons.

Dano, C. and Hicher, P., (2002), "Evaluation of elastic shear modulus in granular materials along isotropic and deviatoric stress paths", 15th ASCE Engineering Mechanics Conference, New York, 1-8.

Dyvik, R and Madshus, C., (1985), "Lab measurement of Gmax using bender elements", Advances in the art of testing soil under cyclic conditions. New York: ASCE: 186–196.

El-Sekelly, W., Mercado, V., Abdoun, T., Zeghal, M., El-Ganainy, H., (2013), "Bender Elements and System Identification for Estimation of V_s ", International Journal of Physical Modelling in Geotechnics, 13(4), 111-121.

Fonseca, A. V., Ferreira, C., Fahey, M., (2009), "A framework interpreting bender element tests, combining time-domain and frequency-domain methods", Geotechnical Testing Journal, 32(2), 91-107.

Ishihara, K., (1996), "Soil Behaviour in Earthquake Geotechnics", Oxford, Oxford science publications.

Jovicic, V., Coop, M.R. and Simic, M., (1996), "Objective criteria for determining Gmax from bender element tests", Géotechnique, 46(2), 357-362.

Karl, L., Haegeman, W., Pyl, L. & Degrande, G., (2003). "Measurement of material damping with bender elements in triaxial cell", In Proceedings of the Third International Symposium on Deformation Characteristics of Geomaterials, Lyon, 1, 3-11.

Kramer, S.L., (1996), "Geotechnical Earthquake Engineering", New Jersey, Prentice Hall.

Lawler, M., (2002), "Estimating the ground deformations associated with earthworks and foundations in boulder clay", Ph.D Thesis, Dept. of Civil, Structural & Environmental Engg., Trinity College Dublin, Ireland.

Lee, J.S. and Santamarina, C., (2004), "Bender elements: performance and signal interpretation", Journal of Geotechnical and Geoenvironmental Engineering", 131(9), 1063-1070.

Lings, M.L. and Greening, P.D., (2001), "A novel bender/extender element for soil testing", Géotechnique, 51(8), 713-718.

Salgado, R., Drnevich, V.P., Ashmawy, A., Grant, W.P., and Vallenas, P.,(1997), "Interpretation of large-strain seismic cross-hole tests", Journal of Geotechnical and Geoenvironmental Engineering, 123(4), 382-388.

Sanchez-Salinero, I., Roesset, J. M., and Stokoe, K. H. (1986). "Analytical studies of body wave propagation and attenuation." Report GR 86-15, Civil Engineering Department, University of Texas at Austin, TX.

Skipper, J., Follett, B., Menkiti, C.O., Long, M. and Clark-Hughes, J., (2005), "The engineering geology and characterization of Dublin Boulder Clay", Quarterly Journal of Engineering Geology and Hydrogeology, 38, 171-187.

Sorensen, K.K., Baudet, B.A., and Simpson, B. (2010), "Influence of strain rate and acceleration on the behaviour of reconstituted clays at small strains", Géotechnique, 60(10), 751-763.

Stasa, F. L., (1985), "Applied Finite Element Analysis for Engineers", New York, CBS College Publishing.

Viggiani, G. and Atkinson, J.H., (1995a), "Interpretation of bender element tests", Géotechnique, 45(1), 149-154.

Viggiani, G. and Atkinson, J.H., (1995b), "Stiffness of fine-grained soil at very small strains", Géotechnique, 45(2), 249-266.

Weidinger, D, M., Ge, L., and Stephenson, R., (2009), "Ultrasonic pulse velocity tests on compacted soil"Geotechnical Special Publication, Characterization, Modeling, and Performance of Geomaterials, 189,150-155.

Yamashita, S., Kawaguchi, T., Nakata, Y., Mikami, T., Fujiwara, T. & Shibuya, S. (2009). Interpretation of international parallel test on the measurement of G_{max} using bender elements. Soils Found. 49, No. 4, 631-650.

Youn, U.J., Choo, Y.W., and Kim, D.S., (2008), "Measurement of small-strain shear modulus G_{max} of dry and saturated sands by bender element, resonant column, and torsional shear tests" Canadian Geotechnical Journal, 45(10), 1426-1438.

List of Figures

Figure 1. An experimental trace for a standard Sine wave input for Chennai marine clay Figure 2. An experimental trace with near-field event for a standard Sine wave input. Figure 3. An experimental trace without near-field event for a distorted Sine wave input.

Figure 4. A representative mesh of the finite element model.

Figure 5. Input for estimation of shear wave velocity through a single Sine wave.

Figure 6. Horizontal deflection of the receiving tip bender element for a single Sine wave input.

Figure 7. Percentage error for the estimation of small strain shear stiffness using a single Sine wave input.

Figure 8. Input for estimation of shear wave velocity through a continuous Sine wave.

Figure 9. Horizontal deflection of the receiving tip bender element for a continuous Sine wave input.

Figure 10. Percentage error for the estimation of small strain shear stiffness using a continuous Sine wave input.

Figure 11. Input for estimation of shear wave velocity through a distorted Sine wave.

Figure 12. Horizontal deflection of the receiving tip bender element for a distorted Sine wave input.